# Toward an optical evidence of quantum interference between macroscopically distinct states

A. Montina[1,*] and F. T. Arecchi[1,2,†]
[1]*Department of Physics, University of Florence, Florence, Italy*
[2]*Istituto Nazionale di Ottica, Largo E. Fermi 6, 50125 Florence, Italy*
(Received 6 April 1998)

Thus far, all proposals for an optical evidence of macroscopic quantum interference have been frustrated by the low detector efficiencies. Two innovations permit such an evidence with currently available equipment. We refer to the generation scheme of entangled states by parametric amplification proposed by S. Song, C. M. Caves, and B. Yurke [Phys. Rev. A **41**, 5261 (1990)]. Setting a low gain for the parametric amplifier introduces a drastic cutoff in the generated photon-number probabilities that compensates for the broadening of the detection probability in the first detector. Furthermore, we supplement the final homodyne detector with a degenerate type-I parametric amplifier which brings nearer the two previously distant states of the superposition. The availability of optical superposition states with large separation suggests a practical way of transforming them into entangled coherent states associated with different paths, thus providing a new convenient source for a ''which path'' experiment. [S1050-2947(98)08011-1]

PACS number(s): 03.65.Bz, 42.50.Lc

The possibility of interference between macroscopically distinct states (the so-called Schrödinger cats [1]) has been suggested by Leggett [2–4] for the case of two opposite magnetic flux states associated with a SQUID (superconducting quantum interference device). References [2–4] refer to MQC (macroscopic quantum coherence) which consists in detecting interference between two states confined in the two valleys of a double-well potential. Thus far, no laboratory evidence of such an effect has been provided.

Recently two experiments on Schrödinger cats have been demonstrated. In the first one [5] the two different states $|\pm\alpha\rangle$ are coherent states of the vibrational motion of a $^9Be^+$ ion within a one-dimensional ion trap. The maximum separation reported between the two states corresponds to about $2|\alpha|=6$. In the second one [6] the two different states are coherent states of a microwave field, with a maximum separation up to about 3.3.

An optical experiment would consist in generating the superposition of two coherent states of an optical field and detecting their interference. Generating a superposition of coherent states requires some nonlinear optical operations, and different proposals have been formulated, based respectively on $\chi^{(3)}$ and $\chi^{(2)}$ nonlinearities. In the first one [7] a coherent state, injected onto a $\chi^{(3)}$ medium, evolves towards the superposition of two coherent states 180° out of phase with each other. However, for all practically available $\chi^{(3)}$ values, the time necessary to generate the superposition state, which scales as $1/\chi^{(3)}$, is always much longer than the decoherence time. We recall that, for a superposition $(|\alpha\rangle+|-\alpha\rangle)/\sqrt{2}$ of two coherent states, the decoherence time is given by the damping time of the field, divided by the square distance $(4|\alpha|^2)$ [7].

The second proposal, by Song, Caves, and Yurke (SCY) [8], consists of an optical parametric amplifier (OPA) pumped by a coherent field, generating an entangled state of signal ($S$) and readout ($R$) modes. Passing the $S$ mode through a further OPA, and measuring its output field conditioned upon the photon number on the $R$ mode, should yield interference fringes, associated with the coherent superposition of two separate states. However, the fringe visibility is extremely sensitive to the $R$ detector efficiency, and as a result the SCY interference has not been observed so far.

Here we propose a modified version of SCY, whereby fringes can still be observed at the efficiencies of currently available detectors. The price to be paid is a very low count rate, which is, however, compensated for by the use of a high-frequency pulsed laser source.

The SCY proposal relies on an experimentally tested quantum nondemolition (QND) scheme [9] in which two correlated field modes with the same frequency and direction but with mutually orthogonal polarizations, generated via a KTP parametric amplifier, are mixed by a subsequent half-wave plate. Our setup is shown in Fig. 1.

The overall evolution operator of the first OPA is the product of operator $U(r)$ describing the parametric amplifier and operator $T(\theta)$ describing the polarization rotator, that is,

$$T(\theta)U(r)=e^{\theta(\hat{a}_R^\dagger\hat{a}_S-\hat{a}_S^\dagger\hat{a}_R)}e^{r(\hat{a}_S^\dagger\hat{a}_R^\dagger-\hat{a}_S\hat{a}_R)} \tag{1}$$

where $r$ is proportional to the product of the pump laser amplitude and the nonlinear susceptibility $\chi^{(2)}$ of the parametric amplifier, $\theta$ is the rotation angle introduced by the half-wave plate, and $S$, $R$ denote the signal and readout modes, respectively.

Choosing the backevasion condition $\sin 2\theta=\tanh(r)$ [9] it can be shown that the state of the two field modes at the output of the QND apparatus is

$$|\psi\rangle=e^{-iT\hat{X}_S\hat{Y}_R}|0,0\rangle, \tag{2}$$

where $T=2\sinh(r)$ [10] and $\hat{X}_S=(\hat{a}_S+\hat{a}_S^\dagger)/\sqrt{2}$, $\hat{Y}_R=(\hat{a}_R-\hat{a}_R^\dagger)/(i\sqrt{2})$.

*Electronic address: almont@ino.it
†Electronic address: arecchi@ino.it

 

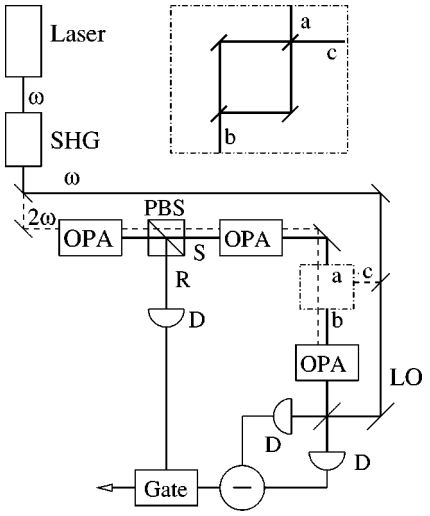


FIG. 1. Layout of the proposed experiment: SHG, second harmonic generation; OPA, optical parametric amplifiers (including polarization rotators); PBS, polarizing beam splitter; *R*, readout channel; *S*, signal channel; *D*, detectors; LO, local oscillator for homodyne. The homodyne detection is performed via a balanced scheme. The dash-dotted box on the *S* channel (magnified in the inset) denotes the optional insertion of a Mach-Zehnder interferometer with two inputs, *a* and *c*, and one output *b*. Branch *c* includes a phase adjustment in order to build the superposition state given by Eq. (18). When no interferometer is inserted, *a* coincides with *b*.

In the representation of the eigenstates $|x_S, y_R\rangle$ of $\hat{X}_S$ and $\hat{Y}_R$, $|\psi\rangle$ is written as

$$\psi(x_S, y_R) = \langle x_S, y_R|\psi\rangle = e^{-iTx_S y_R}\psi_o(x_S, y_R), \tag{3}$$

where $\psi_o(x_S, y_R)$ is the wave function of the vacuum state.

By a photodetection measurement on mode *R*, we obtain the (not normalized) state $\psi_n^S$ of mode *S* conditioned upon the photon number *n* on *R*, that is,

$$\psi_n^S(x_S) = \int_{-\infty}^{\infty} dy_R \psi(x_S, y_R)\psi_n^*(y_R), \tag{4}$$

where *n* is the photon number detected on *R* and $\psi_n(y_R)$ is the number state $|n\rangle$ in the $y_R$ representation of the *R* mode.

The integral

$$P(n) = \int_{-\infty}^{\infty} |\psi_n^S(x)|^2 dx \tag{5}$$

gives the probability that *n* photons are in mode *R*.

The probability distribution of $x_S$, conditioned on the photon number in mode *R*, is [10]

$$P(x_S|n) = \frac{|\psi_n^S(x_S)|^2}{P(n)}$$

$$= \frac{(2n)!!(1+T^2/2)^{(2n+1)/2}}{\pi^{1/2} n!(2n-1)!!} x_S^{2n} e^{-(1+T^2/2)x_S^2}. \tag{6}$$

Both the dependence of $P(n)$ upon *n* [Eq. (5)] and the dependence of $P(x|n)$ upon *x* [Eq. (6)] for *n* between 0 and 10 have been visualized in Figs. 1 and 2 of Ref. [10].

For $n>0$ the conditional probability (6) is approximated by the sum of two Gaussians whose distance increases with *n*. The width of each of the two peaks is smaller than that corresponding to a coherent state. SCY suggested to increase the peak separation by passing the *S* signal through a degenerate OPA, described by the evolution operator

$$U_1(r_1) = e^{-r_1(\hat{a}_S\hat{a}_S - \hat{a}_S^\dagger\hat{a}_S^\dagger)}. \tag{7}$$

The output of this second OPA consists of the superposition of two near-coherent states. When measuring the quadrature $Y_S$ at the output of the second OPA for a fixed photon number *n* detected on the *R* channel, interference fringes should appear as a result of the superposition.

The probability distributions $P(y_S|n)$ of $Y_S$ for *n* that goes from 0 to 10 and for $T=3$ are reported in Fig. 5 of Ref. [10]. Of course, if we sum up several of them with their weights $P(n)$, the interference fringes cancel out. From this fact, it is easily understood how critical the quantum efficiency of the *R* photodetector is.

Let us suppose that the *R* photodetector has an efficiency $\eta_R<1$. For the time being, we refer to a single photomultiplier detector. We have in mind, e.g., the Quantacon 8852, produced by BURLE Electron Tubes, which has a high gain gallium-phosphide first dynode, permitting discrimination of up to five photoelectron events. Selecting the laser wavelength, the quantum efficiency of the photocathode can be $\eta_R=0.05$. If *n* photons impinge on it, the probability of detecting *m* photons is given by the binomial distribution

$$P(m|n) = \binom{n}{m} \eta_R^m (1-\eta_R)^{n-m}. \tag{8}$$

Thus, the probability of $y_S$ conditioned by the detection of *m* photons on *R* is given by

$$P_\eta(y_S|m) = \sum_{n\geqslant m} P(y_S|n)P(n|m) \tag{9}$$

$$= \sum_{n\geqslant m} \frac{P(y_S|n)P(m|n)P(n)}{N(m)},$$

where $P(n)$ is given by Eq. (5) and the normalization factor in the denominator is $N(m)=\Sigma_n P(m|n)P(n)$.

The $P_\eta$ are reported in Fig. 2, using the parameters chosen in [10] ($T=3$), for some values of the efficiency and for *m* that goes from 1 to 5. Already with $\eta_R=0.7$ the fringes practically disappear; therefore no superposition is observed.

The last term of Eq. (9), based on Bayes theorem, says that in order to get the distribution of $y_S$, conditioned by the detection of *m* photons, we must consider all distributions $P(y_S|n)$ for $n\geqslant m$, each one weighted by the probability $P(n|m)$ of *n* photons when *m* of them have been counted. With the parameters considered in [10], $P(n|4)$ has the behavior reported in Fig. 3(a) (we have set $m=4$). The uncertainty on *n* implies a reduction of the fringe visibility on $y_S$.

We aim at reducing the width of the distribution $P(n|m)$, based on the available efficiency of commercial detectors. The only parameter that we can change is the gain *T* of the first OPA. Reducing the value of gain *T*, the distribution $P(n)$ decays faster for increasing *n*. In Fig. 3(b) we have

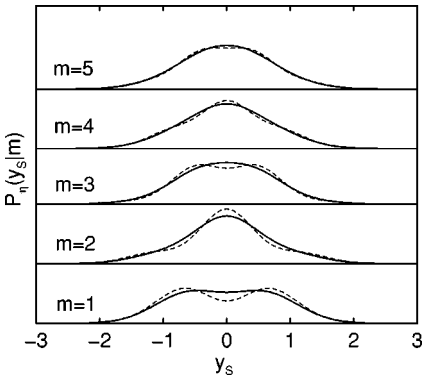


FIG. 2. Probability distribution $P_\eta(y_S|m)$ of $y_S$ for $T=3$ and different efficiencies of the readout detector: $\eta_R=0.7$ (dashed line); $\eta_R=0.5$ (solid line).

reported $P(n|4)$ for $\eta_R=0.3$ and for $T=2$, 1, and 0.4. In this last case we note a sharp reduction of the probability for $n>m$; therefore if the detector counts $m$, there is a very small probability of having $n>m$ photons. To confirm such a guess, we report in Fig. 4 the distributions $P_\eta(y_S|m)$ for some values of $T$ and for $\eta_R=0.3$.

The very remarkable fact is that for $T=0.4$ the fringe visibility is not practically affected by lowering the quantum efficiency. An alternative detection scheme replaces the single photomultiplier with an array of single-photon detectors [11,12]. In such a case the binomial distribution (8) no longer holds, and one should instead return to Eq. (11) of Ref. [11]. This change does not affect the fringe visibility.

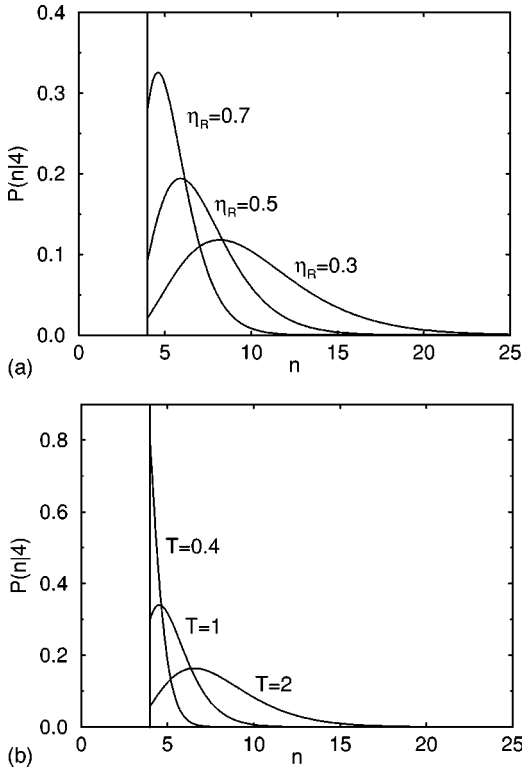


FIG. 3. Conditional probability of an impinging photon number $n$ when the detector registers $m=4$ (a) for different efficiencies $\eta_R$ at a fixed OPA gain $T=3$ (b) for different gains $T$ at a fixed efficiency $\eta_R=0.3$.

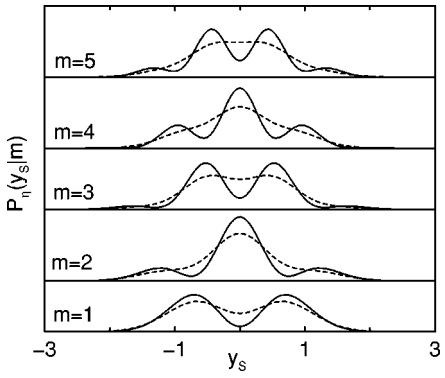


FIG. 4. Same as Fig. 2 but with fixed $\eta_R=0.3$, $T=1$ (dashed line) and $T=0.4$ (solid line).

Lowering $T$ has no practical influence on the separation of the two near-coherent states at the exit of the second OPA for the same photon number $m$ in mode $R$, as we will demonstrate.

The conditional probability distribution $P(x_S|n)$ at the exit of the first OPA [see Eq. (6)] for $n>0$ corresponds approximately to two Gaussian peaks, whose distance and width are $\Delta x=2n^{1/2}(1+T^2/2)^{-1/2}$ and $\sigma=\frac{1}{2}(1+T^2/2)^{-1/2}$, respectively. Therefore the distance to width ratio $\Delta x/\sigma=4\sqrt{n}$ is independent of $T$. The two distributions broaden as they move away from each other, keeping the same distance to width ratio as the starting states [8], thus, the distance of the near-coherent states at the exit of the second OPA depends only on $\sigma$ and $n$. Therefore, putting for $\sigma$ the width $\sigma=1/\sqrt{2}$ of a coherent state, it results that the distance of the two states and the mean photon number at the exit of the second OPA are approximately given by

$$\Delta x_c=4\sqrt{\frac{n}{2}}, \quad \langle \hat{a}_S^\dagger \hat{a}_S\rangle=n. \tag{10}$$

The mean photon number on $S$ is equal to the photon number present on $R$.

We have thus proved that lowering $T$ allows one to solve the efficiency problem of the $R$ photodetector with no change in the final state of mode $S$. However, there is a price to pay, indeed, a small $T$ lowers the probability of photon detection on mode $R$. In Fig. 5 we have reported the distribution $N(m)$,

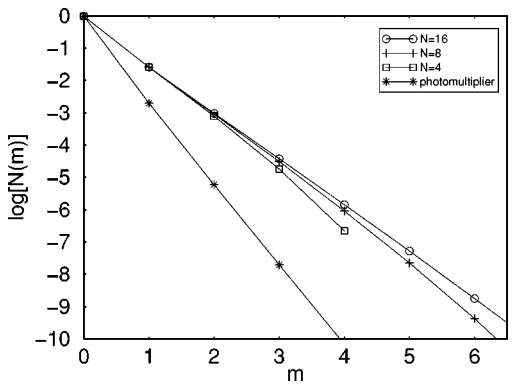


FIG. 5. Log plot of the count probability for $T=0.4$, for a single photomultiplier tube with quantum efficiency 0.05 (line with starred points) and for arrays of $N=4$, 8, and 16 diode detectors.

for $\eta_R=0.05$ and $T=0.4$. $N(4)$ is less than $10^{-10}$; thus, even if we utilize a pulsed laser with frequency 80 MHz and select $m=4$, we have less than one favorable event every 100 s. Thus, we must compromise between the fringe visibility and the counting rate.

A much higher counting rate is obtained by using an array of diodes following the proposal by Paul *et al.* [11,12]. Using that approach, we evaluate the curves reported in Fig. 5. The three curves for $N=4$, 8, and 16 detectors refer to silicon diodes with 0.7 quantum efficiency. For four photons, the count rate is now of the order of $10^{-6}$, thus yielding 20–80 counts/s with a laser pulsed at an 80-MHz rate.

The $Y_S$ quadrature is measured via a homodyne detector. The mode $S$ is superposed to a reference field at frequency $\omega$, with appropriate phase, and we measure the intensity of the superposition.

The following considerations refer to a single arm homodyne scheme. In fact, the used scheme will be a balanced one, as indicated in Fig. 1; however, the results are the same.

In the Heisenberg representation, the coupling of the two fields of mode $S$ and local oscillator LO due to the beam splitter implies the following operator transformation:

$$\hat{b}_S=\tau_b^{1/2}\hat{a}_S+(1-\tau_b)^{1/2}\hat{a}_{\mathrm{LO}},$$
$$\hat{b}_{\mathrm{LO}}=-(1-\tau_b)^{1/2}\hat{a}_S+\tau_b^{1/2}\hat{a}_{\mathrm{LO}}, \tag{11}$$

where $\hat{b}$ denote the operators for the two output fields and $\tau_b$ is the intensity transmittance of the beam splitter. We suppose that $\tau_b$ is close to unity so that the local oscillator does not add large quantum fluctuations to the signal and $(1-\tau_b)^{1/2}\hat{a}_{\mathrm{LO}}$ can be considered as a $c$ number that we denote by $\gamma_{\mathrm{LO}}$. We have then

$$\hat{b}_S=\hat{a}_S+\gamma_{\mathrm{LO}}. \tag{12}$$

Therefore we can write the following transformation law for the wave function $\psi(y_S)$ in the Schrödinger representation:

$$\psi(y_S)\rightarrow e^{-i\sqrt{2}\,\mathrm{Re}[\gamma_{\mathrm{LO}}]y_S}\psi(y_S-\sqrt{2}\,\mathrm{Im}[\gamma_{\mathrm{LO}}]). \tag{13}$$

To detect the fringes we adjust the LO phase so that $\gamma_{\mathrm{LO}}$ is imaginary, and write $\sqrt{2}\ \mathrm{Im}\gamma_{\mathrm{LO}}=A$. The probability that the $S$ detector counts $N$ photons in the resulting field, if its efficiency is 1, is given by

$$P_o(N)=\left|\int_{-\infty}^{+\infty}\langle N|y_S\rangle\psi(y_S-A)dy_S\right|^2. \tag{14}$$

Accounting for the photodetector efficiency $\eta_S<1$, the count probability becomes

$$P_o^{\eta}(M)=\sum_{N\geq M}P_o(N)P(M|N), \tag{15}$$

where

$$P(M|N)=\binom{N}{M}\eta_S^M(1-\eta_S)^{N-M}. \tag{16}$$

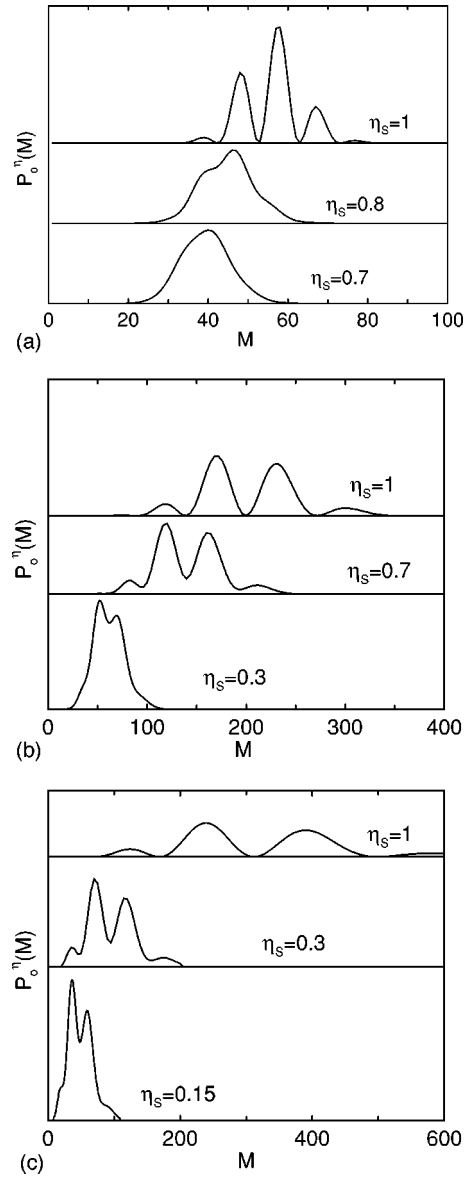


FIG. 6. Photocount distribution after the homodyne detection for an input field of two coherent states $|\pm\alpha\rangle$ where $|\alpha|^2=5$ for different homodyne detector efficiencies $\eta_S$ and with a pre-OPA set at different gains $l$: (a) $l=1$ (no pre-OPA), (b) $l=0.3$, (c) $l=0.15$. The different horizontal scales correspond to different LO intensities for the three cases.

In Fig. 6(a) we report the distributions $P_o^{\eta}(M)$ for some values $\eta_S$ of the homodyne detector efficiency in the case of a superposition of two coherent states of opposite phase with separation $2|\alpha|=2\sqrt{5}$. Already for $\eta_S=0.8$ the fringes are barely visible.

We expect that use of $p$-$i$-$n$ diodes should provide a high detection efficiency [13]. However, we devise a way to improve the fringe visibility as if the efficiency were very close to unity.

$P(M|N)$ has the effect of rounding off the distribution $P_o(N)$. By spreading the distribution $P_o(N)$, it becomes less sensitive to this roundoff. This can be done by incorporating in the detection system a pre-OPA whose role consists in separating the fringes.

Indeed, the decoherence rate is proportional to the square root of the distance between the two states in the phase

plane, thus an auxiliary OPA before the homodyne, with gain less than unity for the $x_S$ quadrature, reduces the separation and therefore reduces the effect of the losses.

If l ($<1$) is the shrinking factor for $x_S$ in the auxiliary OPA, then the probability $P_o(N)$ of Eq. (14) changes to

$$P_o(N)=\left|\int_{-\infty}^{+\infty}\langle N|y_S\rangle\psi[l(y_S-A)]dy_S\right|^2. \qquad (17)$$

The corresponding distributions $P_o^{\eta}(M)$ are reported for $l=0.3$ and 0.15 in Figs. 5(b) and 5(c), respectively for the case $|\alpha|^2=5$. With $l=0.3$ and $\eta_S=0.7$ the fringes are well visible, confirming the validity of the proposed strategy. Notice that Fig. 5 is evaluated for a photon number around 100, for the sake of demonstration; in fact, the experiment is carried out with a much higher LO intensity.

To summarize, the opposite roles of second and third OPA consist, respectively, of putting the two states of the superposition away and then reapproaching them. This means that a measurement done in the intermediate space region would resolve two widely separate states. The setup proposed here is an optical implementation of the ideal experiment suggested for the same purpose by Wigner in the case of two spin-1/2 particles, by use of two Stern-Gerlach apparatuses [14]. The availability of an intermediate spatial region suggests a way of transforming the phase-space separation of the two states of the superposition into a real-space separation. Precisely, we might insert a Mach-Zehnder interferometer between second and third OPA. The two inputs of the first beam splitter are fed respectively by the superposition state $(|\alpha\rangle+|-\alpha\rangle)/\sqrt{2}$ and by a coherent state $|\gamma\rangle$ with $|\gamma|=|\alpha|$ and adjustable phase. By a suitable choice of this phase, the two separate arms $A$ and $B$ of the interferometer have a field given by the superposition [15]

$$|\beta_1\rangle_A|0\rangle_B+|0\rangle_A|\beta_2\rangle_B, \qquad (18)$$

where $|\beta_1|=|\beta_2|=\sqrt{2}|\alpha|$.

Thus, a photodetection performed on the two arms of the interferometer would provide a photon number $2|\alpha|^2$ on one arm and 0 on the other or vice versa; however, if no measurement is performed within the interferometer, the homodyne system at the output will detect an interference between the two alternative paths. Adjusting the two interference arm lengths, we recover the input states at interferometer output. This final measurement is a ''which path'' experiment, upgraded to a packet of $2|\alpha|^2$ photons. So far this experiment had been performed with only one photon, whereas in our setup it is scaled to a large photon number. This scaling may be considered as equivalent to the transition from atom optics to molecular optics [16].

In conclusion, we summarize the distinctive features of the proposed scheme.

(1) It is possible to obviate for the low readout detector efficiency by lowering the first OPA gain. The reduction of the useful count rate is compensated for by pumping the OPA with a high frequency pulsed laser.

(2) As in the SCY proposal, we introduce a large separation between the two alternative states selected by the readout condition via a second OPA. Furthermore, inserting a beam splitter the phase space separation is transformed into a real-space separation allowing a ''which path'' experiment.

(3) We compensate for the limited efficiency of the homodyne detector by bringing the two states closer via the third OPA, which increases the fringe separation, thus retaining evidence of the superposition in the case of low homodyne efficiencies. Notice that the third OPA brings nearer two states whose separation is already conspicuous. Detection of fringes means that the two states once prepared at their maximum separation have not decohered. The physics of the Schrödinger cat takes place after the SCY scheme (first and second OPA), the third OPA being an intrinsic part of the observation apparatus.

This work was partly supported by INFM through the Advanced Research Project CAT.

[1] E. Schrödinger, Naturwissenschaften **23**, 807 (1935).
[2] A. J. Leggett, Prog. Theor. Phys. Suppl. **69**, 1 (1980).
[3] A. J. Leggett (unpublished).
[4] A. J. Leggett and A. K. Garg, Phys. Rev. Lett. **54**, 857 (1985).
[5] C. Monroe, D. M. Meekhof, B. E. King, and D. J. Wineland, Science **272**, 1131 (1996).
[6] M. Brune, E. Hagley, J. Dreyer, X. Maitre, A. Maali, C. Wunderlich, J. M. Raimond, and S. Haroche, Phys. Rev. Lett. **77**, 4887 (1996).
[7] B. Yurke and D. Stoler, Phys. Rev. Lett. **57**, 13 (1986).
[8] S. Song, C. M. Caves, and B. Yurke, Phys. Rev. A **41**, 5261 (1990).
[9] A. La Porta, R. E. Slusher, and B. Yurke, Phys. Rev. Lett. **62**, 28 (1989).
[10] B. Yurke, W. Schleich, and D. F. Walls, Phys. Rev. A **42**, 1703 (1990).
[11] H. Paul, P. Torma, T. Kiss, and I. Jex, Phys. Rev. Lett. **76**, 2464 (1996).
[12] H. Paul, P. Torma, T. Kiss, and I. Jex, Phys. Rev. A **56**, 4076 (1997).
[13] G. Breitenbach, S. Schiller, and J. Mlynek, Nature (London) **387**, 471 (1997).
[14] E. P. Wagner, Am. J. Phys. **31**, 6 (1963).
[15] As a matter of fact, the vacuum state is such only if $|\alpha\rangle$ is an exact coherent state. Since, however, the combination of first and second OPA yields only approximate coherent states, we have a residual probability of nonzero photon detection in what we denoted as the $|0\rangle$ state (the ''empty'' side of the interferometer).
[16] M. S. Chapman *et al.*, Phys. Rev. Lett. **74**, 4783 (1995).